Contract No.:

This manuscript has been authored by Battelle Savannah River Alliance (BSRA), LLC under Contract No. 89303321CEM000080 with the U.S. Department of Energy (DOE) Office of Environmental Management (EM).

Disclaimer:

The United States Government retains and the publisher, by accepting this article for publication, acknowledges that the United States Government retains a non-exclusive, paid-up, irrevocable, worldwide license to publish or reproduce the published form of this work, or allow others to do so, for United States Government purposes.

Large Seasonal Fluctuations of Groundwater Radioiodine Speciation and Concentrations in a Riparian Wetland in South Carolina

Daniel I. Kaplan[a*], Ralph Nichols[a], Chen Xu[b], Peng Lin[b], Chris Yeager[c], Peter H. Santschi[b]

[a] Savannah River National Laboratory, Aiken, South Carolina 29808, United States

[b] Department of Marine Sciences, Texas A&M University, Galveston, Texas 77551, United States

[c] Los Alamos National Laboratory, Los Alamos, New Mexico 87545, United States

* Corresponding author, daniel.kaplan@srnl.doe.gov; 803-761-2672

Key Words: Iodine-129, Organo-iodine, Wetlands, Seasons, Temperature, Speciation

Highlights:

- Seasonal radioiodine concentrations repeatedly fluctuate as much as two-order-of-magnitude
- During summer months, radioiodine and percent organo-iodine increases
- During summer months, groundwater temperature increases and water height decreases
- Cause for seasonal fluctuations due not only to hydrology, but also biogeochemical processes

Abstract:

Recent studies evaluating multiple years of groundwater radioiodine (^{129}I) concentration in a riparian wetland located in South Carolina, USA identified strong seasonal concentration fluctuations, such that summer concentrations were much greater than winter concentrations. These fluctuations were observed only in the wetlands but not in the upland portion of the plume and only with ^{129}I, and not with other contaminants of anthropogenic origin: nitrate/nitrite, strontium-90, technecium-99, tritium, or uranium. This unexplained observation was hypothesized to be the result of strongly coupled processes involving hydrology, water temperature, microbiology, and chemistry. To test this hypothesis, an extensive historical groundwater database was evaluated, and additional measurements of total iodine and iodine speciation were made from recently collected samples. During the summer, the water table decreased by as much as 0.7 m, surface water temperature increased by as much as 15 ºC, and total iodine concentrations were consistently greater (up to 680%) than the following winter months. Most of the additional iodine observed in the summer could be attributed to proportional gains in organo-iodine, and not iodide or iodate. Furthermore, ^{129}I concentrations were observed to be two-orders-of-magnitude greater at the bottom of the upland aquifer than at the top. A coupled hydrological and biogeochemical conceptual model is proposed to tie these observations together. First, as the surface water temperature increased during the summer, microbial activity was enhanced, which in turn stimulated the formation of mobile organo-I. Hydrological processes were also likely involved in the observed iodine seasonal changes: (1) as the water table decreased in summer, the remaining upland water entering the wetland was comprised of a greater proportion of water containing elevated iodine concentrations from the

low depths, and (2) water flow paths in summer changed such that the wells intercepted more of the contaminant plume and less of the diluting rainwater (due to evapotranspiration) and streamwater (as the lower levels promote a predominantly recharging system). These results underscore the importance of coupled processes influencing contaminant concentrations, and the need to assess seasonal contaminant variations to optimize long-term monitoring programs of wetlands.

1. Introduction

1.1. Radioiodine in the terrestrial environment

Radioactive iodine, primarily as ^{129}I and ^{131}I, is inadvertently introduced into the environment through nuclear power plant accidents and the subsurface disposal of nuclear waste (Kaplan et al., 2014a; Neeway et al., 2019). Due to its high perceived mobility in the terrestrial environment, large inventory, high bioaccumulation factor through the food chain and human thyroid, ^{129}I is a key risk driver at many Department of Energy disposal facilities in the United States (Fuge and Johnson, 1986; IAEA, 2007; Liu and von Gunten, 1988; Wagner et al., 2012). The U.S. Environmental Protection Agency's Drinking Water Standard (DWS) is 0.037 Bq/L, which is among the lowest of any radionuclide (EPA, 2001). The major species of iodine in the terrestrial environment are iodide (I^-), iodate (IO_3^-), and numerous forms of organo-iodine (org-I) species (Kaplan et al., 2014a). In low organic matter areas, such as in vadose zones or aquifers, iodide sorption is largely controlled by the presence of pH-dependent charge minerals, such as Fe- and Mn-hydroxides (Emerson et al., 2014). As pH decreases in these minerals, anion

adsorption or complexation increases, and at pH levels above the point where the Fe- and Mn-oxides have a net-zero charge, negligible amounts of sorption is measured (Emerson et al., 2014; Fuge and Johnson, 1986). In high organic matter sediments, such as those from wetlands, iodide sorption can be as much as 100x greater than nearby low organic matter sediments (Emerson et al., 2014). In wetland groundwater, org-I, primarily as aromatic and methylated species, may account for >90% of the aqueous iodine in the system, whereas in much lower organic matter systems (OC <0.1%), such as in the vadose zone or subsurface aquifers, org-I species still exist (commonly <20% of total iodine) but inorganic iodine species are more prevalent (Moulin and Moulin, 2001; Shimamoto et al., 2011; Xu et al., 2011a; Xu et al., 2011b; Xu et al., 2016; Yamaguchi et al., 2010; Zhang et al., 2013). Natural organic matter provides high concentrations of positively charged electrostatic exchange sites, and more importantly, covalent bonding sites where bonds are formed through electrophilic substitution of aromatic structures (Moulin and Moulin, 2001; Xu et al., 2013).

1.2. Seasonality of contaminants in groundwater

Seasonal changes in streamwater contaminant concentrations have been attributed primarily to changes in hydrological/meteorological processes (Benner et al., 2008; DOE-LM, 2012; Meyer et al., 2019; Smith et al., 2010; Yabusaki et al., 2008). Elevated contaminant stream concentrations at elevated water levels may result from the water contacting more of the surrounding contaminated stream banks and associated aquifer/vadose zone (Yabusaki et al., 2008). This was observed on the Department of Energy's Hanford Site in Washington, USA in response to seasonal snow melts causing the Columbia River levels to rise and in turn cause the

adjacent groundwater levels to rise into the uranium contaminated vadose zone. Conversely, increased contaminant concentrations at lower water levels have been attributed to evaporation of smaller streams in arid regions, thereby concentrating contaminants in the small streams flowing through arid regions (DOE-LM, 2012).

Seasonal changes in contaminant concentrations have less commonly been attributed to concurrent changes in contaminant speciation. During a 1-year study conducted in an unconfined groundwater system in a semi-arid region of Cyprus, dissolved uranium was reported to be a minimum (387 mBq/L) during October when rainwater infiltration was greatest (Efstathiou et al., 2014). They attributed the lower total U groundwater concentrations to U(VI) being reduced to the less soluble form of U(IV) and to dilution. Once the weather become hot and dry between May and September, total U concentrations increased due to reoxidation of the U to the more soluble U(VI) form, plateauing at about 730 mBq/L. Similarly, Kumar and Riyazuddin (2011) noted that total selenium concentrations in drinking water increased during the post-monsoon period due to the oxidation of the sediment-bound Se(IV) to dissolved Se(VI). Several studies have shown seasonal changes in arsenic concentration, resulting from coupled hydrological/meteorological induced changes in arsenic speciation (Ayotte et al., 2015; Benner et al., 2008; Berg et al., 2001; Nadakavukaren et al., 1984; Polizzotto et al., 2008; Schaefer et al., 2016). Schaefer et al. (2016) observed that during periods when groundwater oxygen and/or nitrate levels were greatest during the rainy season, that arsenic concentrations decreased, but not proportionally to oxygen concentration. After the rainy season, when the recharge period subsided, low-redox and low-arsenic conditions were re-established by natural humic substances. Strong seasonal shifts in groundwater arsenic concentration were attributed to shifts in rainfall and hydrologic gradients that induced sharply contrasting redox and organic matter conditions in

114 the aquifer (Polizzotto et al., 2008). In Nevada, Thundiyil et al. (2007) reported significant
115 seasonal changes in arsenic concentrations, but the significant changes were not consistent
116 between wells. Some locations showed increased arsenic concentrations during the dry season
117 while others showed significant increases during the wet season.
118
119 *1.3. Radioiodine in F- and H-Areas, Savannah River Site*
120
121 The Savannah River Site is in South Carolina, USA and borders the Savannah River (Fig. 1).
122 The F- and H-Areas on the Savannah River Site were facilities used to separate radionuclides for
123 nuclear weapons and nuclear heat sources (SRNS, 2019). During operations, 7 billion liters of
124 predominantly acidic aqueous waste were disposed in unlined disposal basins from 1955 until
125 1988. The waste contained several metals (including Cd, Hg, and Pb) and radionuclides
126 (including ^{3}H, and ^{129}I and multiple isotopes of U, Pu, Sr, and Cs). In 1988, the basins were
127 closed by removing most of the waste, back filling the basins with slag, limestone, and sediment,
128 and then covering the basins with a low-permeable clay closure cap. Radionuclides have entered
129 the underlying aquifer and are moving south towards Fourmile Branch (Fig. 1). Approximately
130 7×10^{10} Bq ^{129}I was disposed in F-Area, and 1×10^{10} Bq ^{129}I in the H-Area (Killian et al., 1987a,
131 b). The mobility of iodine is greatly dependent on its speciation, such that a ranking of iodine
132 species based on their mobility in soils is generally: $I^- > IO_3^- >$ org-I (Emerson et al., 2014;
133 Schwehr et al., 2009; Xu et al., 2011a; Zhang et al., 2011). Iodine speciation in the terrestrial
134 environment is influenced primarily by pH (Emerson et al., 2014; Xu et al., 2011a), sediment
135 redox state (Emerson et al., 2014), the presence of natural organic matter (Xu et al., 2013; Xu et
136 al., 2011a; Xu et al., 2012), and microbial activity (Li et al., 2012a; Li et al., 2011; Li et al.,

2012b; Yeager et al., 2017). Accelerator Mass Spectrometry measurements of $^{129}I/^{127}I$ ratios in the plume demonstrated that the speciation of ^{129}I and ^{127}I were similar for I^-, IO_3^-, and org-I (Schwehr et al., 2014). The $^{129}I/^{127}I$ atom ratios ranged from 0.176 in the plume to 0.003 in adjacent areas outside the plume. The similarity of speciation between aqueous ^{129}I and ^{127}I was also observed through wet chemistry techniques by Otosaka et al. (2011).

Denham and Amidon (2016) conducted concentration trend analyses of a half dozen radionuclides in 45 locations (upland wells, wetland wells, and surface water streams) in the F- and H-Areas. Trends of the historical ^{129}I concentration data, dating back to as early as 1993, typically did not show a discernable statistical trend when plotted against time. However, seven locations in the wetlands showed decreasing ^{129}I concentration trends with environmental half-lives (the time required for ^{129}I groundwater concentrations to decrease by half) that ranged from 2.7 to 19 years. These decreasing concentrations were attributed to dilution and binding to the low-pH (pH 2.9 to 5.5), high natural organic matter sediments, but not to radiological decay (^{129}I has a half-life of 16Ma years). Building on the results of Denham and Amidon (2016), Nichols and Dickson (2020) conducted a similar time-trend analysis but focused their attention on 13 wetland locations, and showed that aqueous ^{129}I concentrations at various locations were either significantly increasing or decreasing. While the decreasing concentration trends were expected, they proposed that the increasing concentration trends could be attributed to the wetlands acting in a manner similar to that of a chromatography column that had been receiving low levels of ^{129}I for decades and was now slowly releasing elevated concentrations.

Overall, the most intriguing facet of these two studies was the consistent and significant seasonality trends observed at some wetland locations, whereby ^{129}I water concentrations consistently increased during the summer. For this study, our working hypothesis was that there

160 are multiple processes interacting to produce this response, including hydrology, water
161 temperature, microbiology, and chemistry. The objectives of this study were three-fold: (1) to
162 determine correlations between historic aqueous ^{129}I concentration, water table height,
163 temperature, and other radionuclide concentrations, (2) create a depth profile of ^{129}I
164 concentrations along a transect in the upland portion of the contaminant plume, and (3) examine
165 changes in iodine speciation as a function of seasons. Our general approach was to gather
166 additional information to identify and qualitatively describe the important field scale processes
167 governing the observed ^{129}I seasonal trends. Such information can be used to improve
168 subsequent calculations of radiation dose originating from the study site.
169

170 ## 2. Materials and Methods

171

172 *2.1. Study Site and Field Sampling*

173

174 The Savannah River Site has a semi-tropical climate that receives an annual rainfall of 122
175 cm/year that is evenly distributed throughout the year. It is in the Atlantic Coastal Plains that was
176 formed from fluvial, deltaic, and shallow marine deposits of sediment (Denham, 1995). In F- and
177 H-Areas, the unconfined aquifer is in the Eocene Dry Branch Formation and has an average
178 thickness of about 10 m and hydraulic conductivity ranging from 104 to 143 m/yr (SRNS, 2019).
179 Underlying the unconfined aquifer within the Dry Branch Formation is a low permeability, non-
180 continuous Tan Clay layer that ranges from 0 to 2.5 m in thickness. Since the disposal basins
181 were closed in 1988, several remediation approaches have been implemented that influenced the
182 hydrology and water chemistry in various regions of the study site, including a short-lived pump-

and-treat program, a base-injection program, and a silver chloride injection demonstration (Denham and Vangelas, 2008; SRNS, 2019).

2.1.1. Long-term trends of surface water monitoring of ^{129}I

The data used to evaluate long-term trends of groundwater ^{129}I concentrations were part of the Savannah River Site's radionuclide monitoring program. The purpose of this monitoring program is address state and federal regulations and to assess the risk posed by the ^{129}I. While the water-quality monitoring program in the F- and H-Areas go back to the 1980s, routine quarterly monitoring (sampling every 3 months) for the specific wetland locations used in this study were only initiated in 2010. Occasionally there were additional field duplicates and *ad hoc* samples collected for quality control purposes. The criteria for selecting the five surface water locations were that they needed to be in the wetland and needed to show seasonal variations in ^{129}I concentrations. The data is compiled in the SRS's Bechtel Environmental Integrated Data Management System (BEIDMS©).

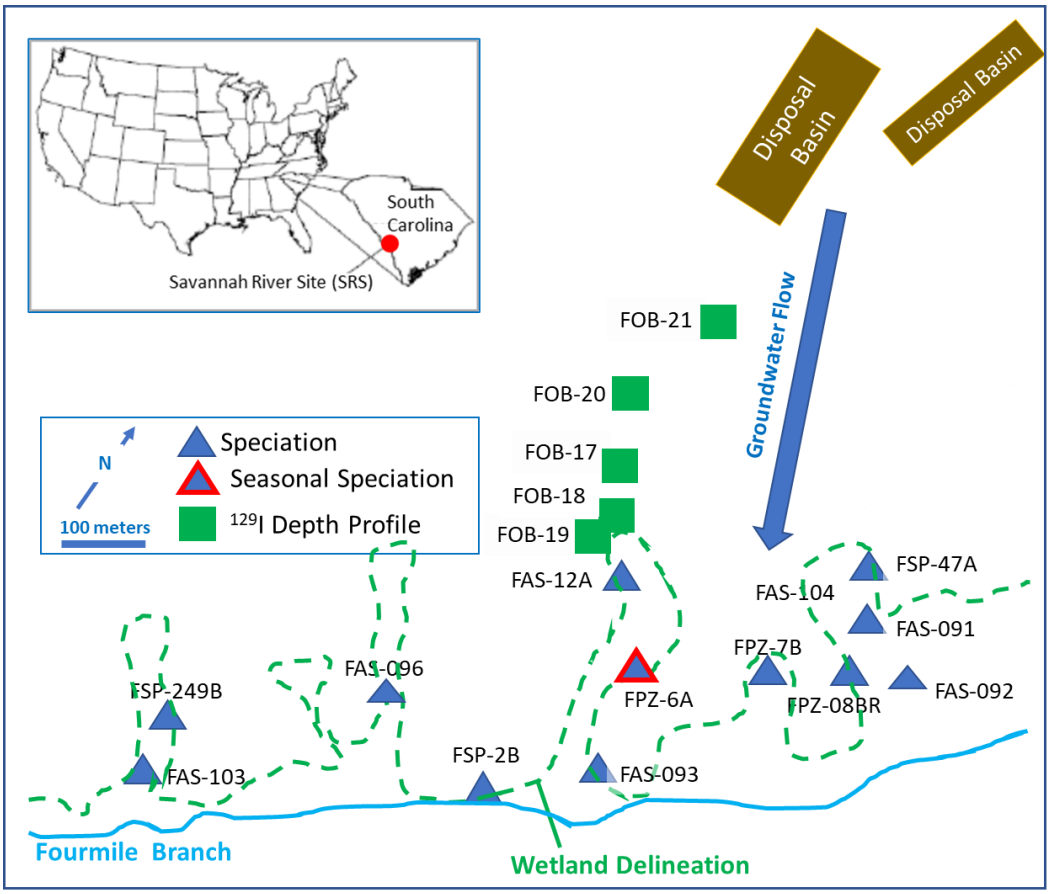

Fig. 1. Sample locations in F-Area for the seasonal iodine speciation study (blue + red diamonds; sampled 10 times between January 2010 to April 2018), iodine speciation study (blue diamonds; sampled once during April 2018) and ^{129}I depth profile study (green squares; sampled once during April 2019). Wetlands are delineated from the uplands by the green dashed line. Disposal Basins are the source of the ^{129}I, and the contaminant plume is migrating in a southerly direction towards Fourmile Branch. Not shown are two wells located in the H-Area plume (HAS-102 and HAS-103) that are approximately 0.6 km east of F-Area (map shown in Supplemental Material; Figure S1).

2.1.2. Total ^{129}I distribution versus aquifer depth

The impetus for investigating ^{129}I concentration as a function of depth was that changes in water table height may alter flow rate and flow direction. Previous studies have reported that pH decreases and specific conductivity increases in a systematically manner with depth in this unconfined aquifer, suggesting that contaminant concentration may also change with depth (Denham and Amidon, 2016). Five well clusters, penetrating at varying depths into the surface

aquifer, along a transect running somewhat parallel with groundwater flow were sampled (Fig. 1; FOB-17, -18, -19, -20, and -21).

2.1.3. Spatial distribution and seasonal changes in aqueous iodine speciation

Triplicate water samples were collected from eleven locations in the F-Area wetland during April 2018 (Fig. 1). These samples were analyzed for iodine speciation, including I^-, IO_3^-, and org-I. Unfiltered water was pumped up slowly from the wells into acid-washed 40-mL glass bottles, stored on ice in the field, and then frozen and stored at -20 ºC until analyzed for iodine speciation.

Among these 11 locations was well FPZ-6A, which was sampled and analyzed for iodine speciation seven previous times over the course of eight years (Otosaka et al., 2011; Zhang et al., 2014). The iodine speciation data from these previous studies were combined with those from this study to statistically evaluate if changes in iodine speciation were seasonal.

2.2. Measurement of iodine species

Total ^{129}I concentrations in groundwater was measured by standard gamma detection methods (Method EPA 901.1) (EPA, 2009). The purpose of these measurements was primarily to address regulatory requires for monitoring the impact of Savannah River Site operations on environmental quality. Briefly, iodine in the aqueous sample was first converted to iodide by adding sodium meta-bisulfite and then recovered from solution with an anion resin. ^{129}I concentrations on the resin were counted using 29-40 keV x-rays by low energy x-ray gamma spectroscopy. Standards were included to permit corrections for self-absorption within the

sample during analysis. The total ^{129}I detection limit was ~0.0185 Bq/L for a 1.5-L water sample. EPA-approved analytical methods (EPA, 2019a, b) were used to measure pH, nitrate/nitrite as nitrogen, depth to water, temperature, ^{90}Sr, ^{99}Tc, ^{3}H, and ^{238}U.

Iodide, iodate, and organo-iodine measurements were conducted as described by Zhang et al. (2010). This method is based on the highly selective transformation of iodide by N,N-dimethylaniline to become 4-iodo-dimethylaniline and subsequent detection of the complexed iodide species by GC–MS. Each groundwater sample was split into three aliquots and full speciation analysis of iodide, iodate and organo-I was performed as follows. Iodide concentrations were measured directly from the as-received sample (1st aliquot) after passing through a 0.45 μm membrane. Iodate concentrations were measured with the second aliquot by adding sodium meta-bisulfite to reduce the iodate to iodide; this sample provided a direct measure of total inorganic iodine and an indirect measure of iodate ([iodate] = [total inorganic iodine] – [iodide]). Total iodine was measured in a third aliquot by first combusting the sample at 900 ºC, followed by reduction with sodium meta-bisulfide. Organo-iodine concentrations were calculated from the total iodine and total inorganic iodine concentrations ([organo-iodine] = [total iodine] – [total inorganic iodine]). Liquid:liquid extraction were carried out with cyclohexane. The detection limit of the method was ~0.04 μg/L (0.07 Bq/L ^{129}I).

2.3. Measurement of standard aqueous analytes

In addition to the various iodine species, several other aqueous analytes were measured following approved standard methods (Baird et al., 2017). Conductivity, dissolved oxygen (DO), temperature, pH, turbidity, and oxygen-reduction potential (ORP) were analyzed in the

261 field using a multiprobe system (YSI, ProDSS Handheld Multiparameter Instrument, YSI
262 Incorporated, Yellow Springs, OH). Ion Chromatography (Dionex Easion IC System, Thermo
263 Fisher Scientific, Waltham, MA) was used to measure the anions, nitrate-N and nitrite-N, by the
264 EPA standard method 300.0. Total alkalinity, carbonate, and bicarbonate were determined by
265 titration following EPA standard method 310.1. Total organic carbon (TOC) was determined by
266 high temperature catalytic oxidation with non-dispersive infrared (NDIR) detection following
267 standard method SM-5310B (Shimadzu TOC-L, Columbia, MD). Related, dissolved organic
268 carbon (DOC) is the organic carbon in the <0.45 μm fraction of a water sample. Finally, cations
269 were measured by Inductively Coupled Plasma – Optical Emission Spectroscopy (Agilent 5800
270 ICP-OES; Santa Clara, CA) following EPA standard method SW846-6010C.
271
272 *2.4. Data retrieval and statistical analysis*
273
274 The database management system used to evaluate historical seasonal trends of total ^{129}I
275 concentrations in the F-Area riparian wetland was the Bechtel Environmental Integrated Data
276 Management System (BEIDMS©). The data in BEIDMS goes back to 1984 and contains
277 approximately 60 million records related to measurements made of environmental samples from
278 the Savannah River Site.
279 The data retrieved from BEIDMS was analyzed using the graphing and statistical software R
280 (R Core Team, 2021; R Core Team and Contributors Worldwide, 2021). Prior to conducting
281 regression analysis, the Cook's distance statistic was estimated to identify data with large
282 residuals, that is, to identify outliers. The historical F-Area groundwater samples were collected
283 over decades, by many operators, and analyzed by multiple chemical analytical labs. The

Cook's distance statistic is a combination of each observation's leverage and residual value. The higher the leverage and residuals, the higher the Cook's distance. Briefly, the value is calculated by removing the i^{th} data point from the model and recalculating the regression. It summarizes the extent to which all the values in the regression model change when the i^{th} observation is removed. The threshold Cook's distance was set to 0.2, resulting in 0 to 3 (0 to 6%) of the data being disqualified from a single well. Disqualifying outliers identified through this method did not consistently increase or decrease correlation coefficients.

The Student's t-Test was used to determine whether iodine speciation was significantly different in the summer (April through October) versus in the winter (December through March).

3. Results and Discussion

3.1. Temporal changes in surface water radioiodine concentrations

^{129}I concentration trends at the five locations investigated between 2010 and 2018 had maximum concentrations generally in September and minimum concentrations in March (Fig. 2). The trend is highly repeatable and occurs in each of the 6 to 8 years of data. These seasonal fluctuations in ^{129}I concentrations could be as much as 16.2 Bq/L (i.e., 680% greater in Well FAS-093 during the summer of 2012 (19.6 Bq/L) than in the following winter (3.4 Bq/L) (Fig. 2). To put this fluctuation in perspective, it is 438 times greater than the Environmental Protection Agency's Drinking Water Standard (DWS) is 0.037 Bq/L (EPA, 2001). Four of the locations showed a decline in ^{129}I concentration over this period. In contrast, FAS-96, showed a clear and consistent increase in ^{129}I concentration over this period. Similarly, Nichols and

Dickson (2020) reported several of the 13 Fourmile Branch wetland locations had increasing ^{129}I concentrations over the past 10 to 15 years.

Similar seasonal fluctuations were not noted in NO_3^-/NO_2^- as N, ^{90}Sr, ^{99}Tc, ^{3}H, or ^{238}U concentrations. A typical example of this data is presented in Fig. 3 (Additional data are presented in Nichols and Dickson (2020) and Denham and Amidon (2016)). Tritium and NO_3^-/NO_2^- as N (the N originates primarily from HNO_3 waste that was disposed along with the radionuclides) are generally regarded as conservative tracers that move freely with water with little interaction with the sediment matrix. The behavior of these two contaminants as conservative tracers in the F-area subsurface is supported by the similarity in their concentration patterns over time (Fig. 3). Since consistent seasonal fluctuations were not observed for the concentrations of these conservative tracer contaminants, it is likely that hydrological changes were not the only process governing the fluctuations of ^{129}I concentrations at this site. Conversely, ^{90}Sr and ^{238}U are very surface reactive in Savannah River Site sediments (Kaplan, 2021), and they too did not show a consistent seasonal change in concentrations. It is noteworthy, that tritium and ^{90}Sr have relatively short half-lives of 12.3 and 28.8 years, respectively, and a significant fraction of their decline over the period of interest may be attributed to radiological decay. ^{99}Tc, ^{129}I, and ^{238}U have extremely long half-lives of 0.2, 16.1, and 4,500 million years, respectively, and therefore detected change in their concentrations cannot be attributed to radiological decay.

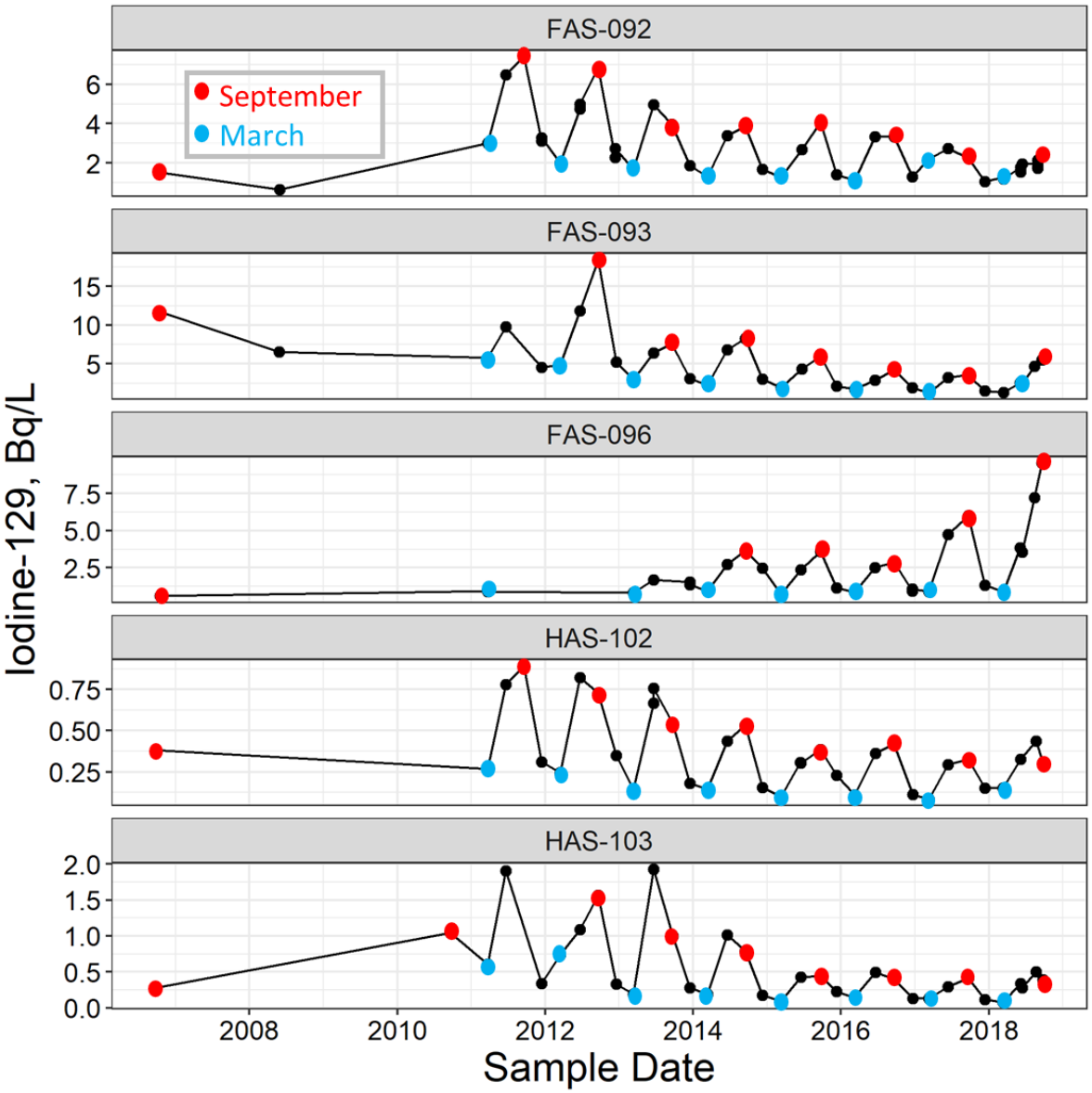

Fig. 2. Seasonal fluctuations of ^{129}I activity concentrations over multiple years in the Fourmile Branch wetland. Red and blue dots represent samples collected in September and March, respectively. Black dots represent samples collected on other months. Note that the y-axis for ^{129}I concentration has a different scale for each well. Data is from the SRS's Bechtel Environmental Integrated Data Management System (BEIDMS©).

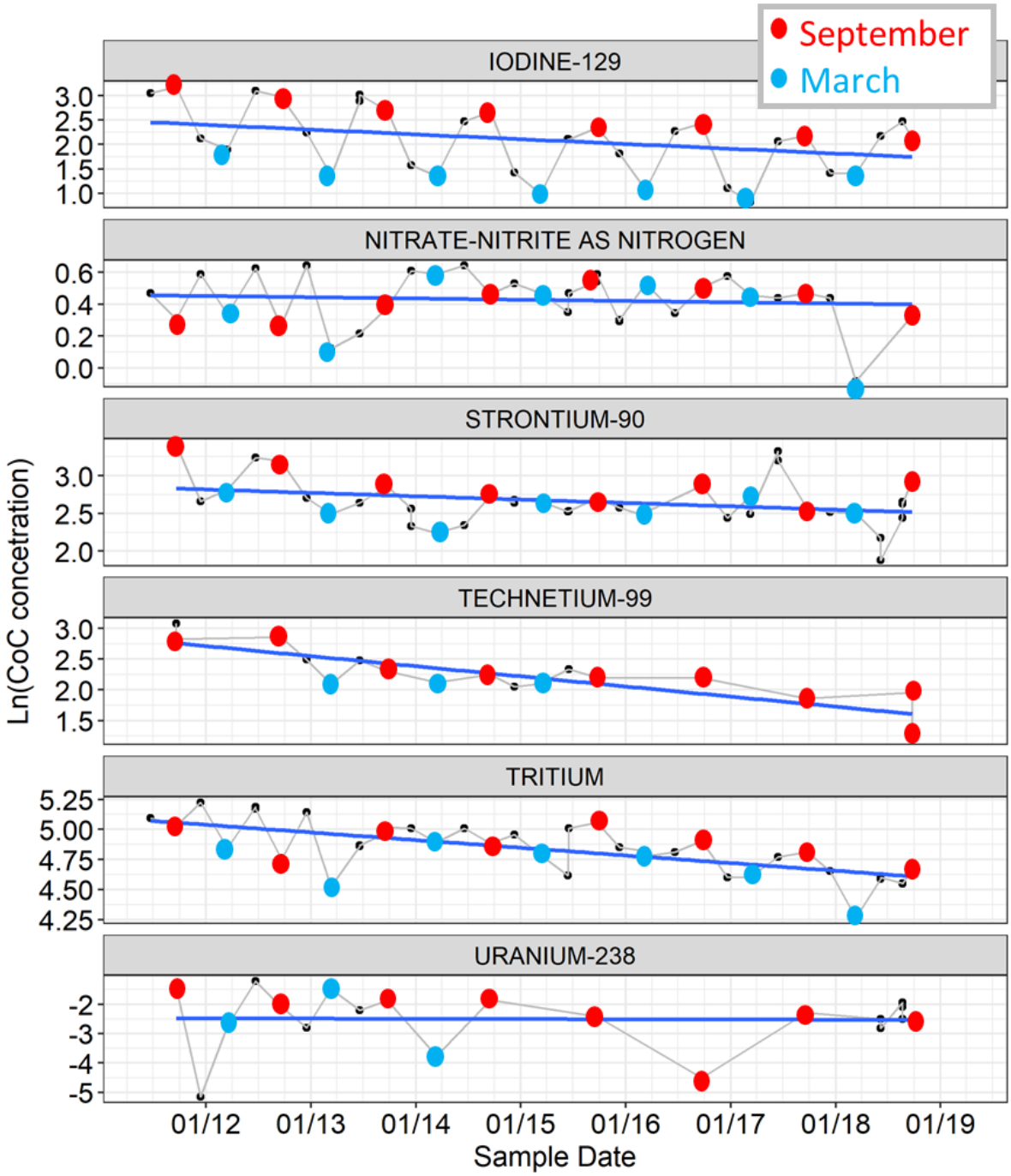

Fig. 3. Example of natural logarithm of the ^{129}I, N, ^{90}Sr, ^{99}Tc, tritium, and ^{238}U activity concentration (Bq/L; Ln(CoC concentration)) in location HAS-102 versus sample date. The blue linear regression line is provided to highlight the overall data trend for the 7 to 8 years of data. To emphasis the seasonal trend for the iodine-129 data, the September samples are identified with red dots, the March samples in blue dots, and other samples are in black dots. Data is from the SRS's Bechtel Environmental Integrated Data Management System (BEIDMS©).

343 *3.2. Temporal changes in iodine speciation*

344

345 Iodine-127 speciation was analyzed in groundwater samples recovered from Well FPZ-6A 10
346 times between January 2010 and April 2018, five times during winter months (December
347 through March) and five times during summer months (April through October) (Table 1). These
348 categories were assigned based on water temperatures. These 10 measurements include seven
349 previously reported data (Otosaka et al., 2011; Zhang et al., 2014) and three new data originating
350 from this study. The generally low pH values and high nitrate concentrations in these samples
351 originates from the large volumes of HNO_3 waste added along with the radionuclides to the
352 Disposal Basins (Table 1). Total iodine concentrations and percentage of org-I were
353 significantly ($p \leq 0.05$; $n = 5$) greater in the summer months than in the winter months. The
354 greater total iodine concentration in the summer months can be attributed primarily to greater
355 org-I. The cause of the greater org-I during the summer months is not known. One possible
356 explanation is that the higher temperatures in the summer may be promoting microbial activity
357 that in term may be directly facilitating dissolved org-I formation, and indirectly facilitating org-I
358 formation by degrading soil-bound organic matter and promoting the release of soil-bound org-I
359 (Li et al., 2012a; Li et al., 2011; Li et al., 2014; Li et al., 2012b). This second mechanism for org-
360 I formation was reported by Biester et al. (2006). They observed that the dominant form of
361 iodine in peatlands was org-I and that dissolved iodine concentrations depended on the degree of
362 peat degradation. Soil organic matter in wetlands is a strong sorbent for iodine (Emerson et al.,
363 2014; Kaplan et al., 2014b; Santschi et al., 2017; Xu et al., 2011a; Xu et al., 2011b; Xu et al.,
364 2016; Xu et al., 2012). While a slight increase in dissolved organic carbon (DOC)
365 concentrations was noted in the summer months (Table 1), significant ($p \leq 0.05$) correlations

between these parameters were observed in a more robust survey of iodine speciation and water chemistry (described in Section 3.5). There are potentially offsetting microbial processes influencing DOC concentrations, namely the microbes remove DOC by metabolizing it for energy and they also create DOC by various processes including breaking down soil-bound organic matter (Sollins et al., 1996). Potentially equally important is that elevated water temperatures may have also promoted diffusion of iodine from sediments (Satoh and Imai, 2020).

Table 1
Seasonal changes in ^{127}I speciation and water chemical properties (samples collected from Well FPZ-6A between 2010 and 2018; $n = 5$; mean ± standard deviation).

	pH	DOC[(a)]	DO[(a)]	ORP[(a)]	Nitrate	Total I	Iodide	Iodate	Org-I
		(mg/L)	(mg/L)	(mV)	(mg/L)	(µg/L)	(wt-%)	(wt-%)	(wt-%)
Winter[(b)]	4.14 ± 0.65	0.40 ± 0.11	2.58 ± 1.7	493.8 ± 42.8	158.9 ± 66.2	14.7 ± 6.2	35.6 ± 13.8	44.7 ± 21.2	19.7 ± 10.3
Summer	4.00 ± 0.22	0.49 ± 0.23	1.43 ± 0.9	449.0 ± 75.8	417.7* ± 135.3	73.4* ± 50.2	24.2 ± 21.7	31.1 ± 8.5	44.7* ± 14.6

[(a)] DOC = dissolved organic carbon, DO = dissolved oxygen, ORP = oxidation-reduction potential.
[(b)] Winter = December through March; Summer = April through October; these definitions of the two seasons were based on water temperature data.
* Indicates a significantly ($p \leq 0.05$; $n = 5$) greater value according to the two-sample t-Test assuming equal variance.

3.3. Radioiodine, water table height, and temperature

Water table height and temperature may be indirect factors influencing ^{129}I concentrations. Temperature influences microbial activity (Roszak and Colwell, 1987) and rate of reactions (Cotton et al., 1988), whereas water table height influences many factors, including volume of the contaminated vadose zone in contact with water, dilution, rate of water movement, and direction of water movement. There was historical temperature data for the surface water

sampling locations and depth-to-water data in nearby groundwater wells for each sampling location showing the seasonal ^{129}I concentration trends (Fig. 4). Depth-to-water is a measure of the distance from the top of the wellhead to the water table, as such it provides an inverse measure of the water table height. In all cases, temperature was significantly and positively correlated to ^{129}I concentrations (Fig. 4, Supplemental Material Table S1).

^{129}I concentrations were also positively and significantly correlated to depth-to-water values (Fig. 4, Supplemental Material Table S1). Stated differently, ^{129}I concentrations increased as the water level decreased. This trend rules out the process that the summer increases in concentration are attributable to elevated water levels promoting ^{129}I desorption as it saturated a larger portion of the contaminated vadose zone. Such a mechanism has been attributed to the release of U from the Hanford Site in eastern Washington state (Yabusaki et al., 2008). They explained that as the Columbia River level rose in response to spring snow melts and then dissolved U levels increases as a result of the water coming into contact with U-contaminated vadose zone sediment. Not surprisingly, depth-to-water and temperature values for all three wells were also correlated to each other because water levels in these wetlands decrease during the summer (data not shown). It is therefore important not to over interpret these parameters as independent of each other; they are changing as co-variants in a manner that was not teased apart from this dataset. Furthermore, these results are simple correlations that are devoid of causality.

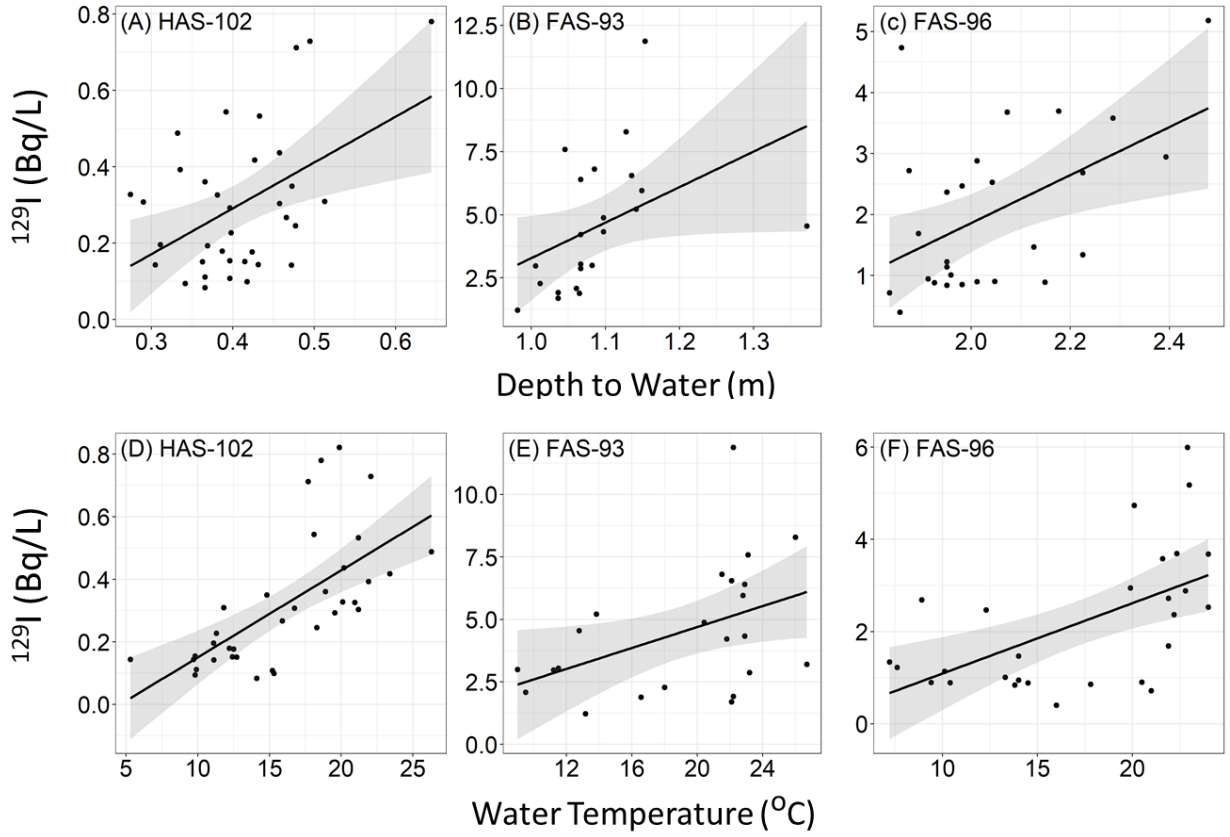

Fig. 4. Groundwater ^{129}I concentrations of three wells versus depth-to-water (**A, B, C**), and water temperature (**D, E, F**). Data were generally collected every 3 months over 6 to 8 years. Gray shaded area represents the 95% confidence interval. Correlation coefficients (r) and level of significance is provided (* represents $p \leq 0.05$ and ** represents $p \leq 0.01$).

3.4. ^{129}I depth profiles in the F-Area plume

As seasonal water levels change in an aquifer, flow patterns and flow rates may also change. If a contaminant plume has a contaminant concentration gradient with depth, then it is possible that as the water table lowers during the summer that the water at lower depths may contribute a greater percentage of the water entering the wetland. An ^{129}I depth profile was measured in the upland portion of the plume entering the Fourmile Branch wetland (Fig. 5). There were 22 ^{129}I samples collected from five wells that each had four or five depths. The ^{129}I concentrations

ranged from <0.019 to 9.18 Bq/L. There was a general trend showing a steep increase in ^{129}I concentrations from the surface of the water table down to the stratigraphic clay layer at the bottom of the aquifer, referred to as the Tan Clay. These results are consistent with the previous observation by Denham and Amidon (2016) who described the most contaminated portion of the plume based on pH and electrical conductivity measurements as approximately 3-m high and moving along the top of the Tan Clay Layer. This vertical gradient may have implications related to why ^{129}I concentration increase when the water table lowers during the summer (Fig. 4); a greater percentage of the water entering the wetland during the summer may originate from the lower layers of the aquifer with elevated ^{129}I concentrations.

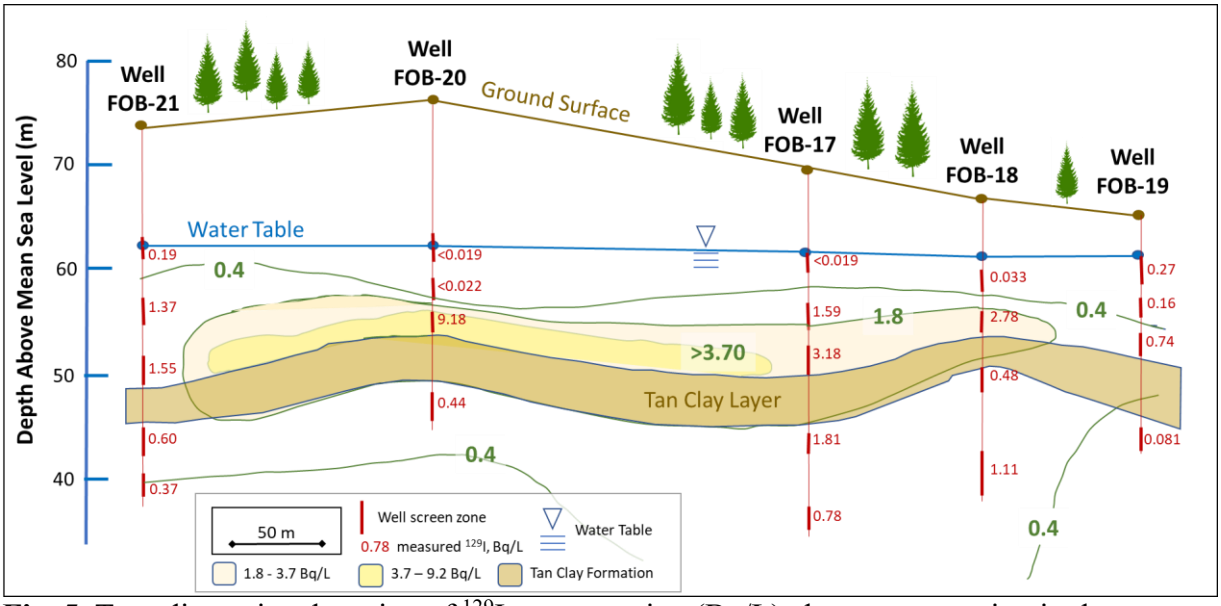

Fig. 5. Two-dimensional section of ^{129}I concentration (Bq/L) along a transection in the contaminant plume upland of the Fourmile Branch wetlands. Well locations are presented in Fig. 1. The depth-discrete ^{129}I concentrations are presented in red font in units of Bq/L. The horizontal and vertical distance scales differ. Samples were collected April 2019. The ^{129}I Drinking Water Standard (DWS) is 0.037 Bq/L (EPA 2001). The Tan Clay Layer is located within the Dry Branch Formation.

3.5. Spatial variation in iodine speciation

Surface water and groundwater samples were collected in April 2018 and analyzed for stable ^{127}I and radioactive ^{129}I speciation. To put these measurements into geochemical context, additional parameters were also measured, including pH, oxidation-reduction potential (ORP), DOC, total N, dissolved Fe, alkalinity, nitrate, tritium, and turbidity. While both ^{127}I and ^{129}I speciation were measured, the former is reported in Fig. 6, because 1) there were several points below detection limit for the ^{129}I dataset, 2) there were large quantities of ^{127}I introduced in the waste as an impurity of the HNO_3 and as part of operations to promote the reduction of Pu(III) to metallic Pu (Orth, 1963; Otosaka et al., 2011), and 3) the speciation of the two isotopes were similarly in this plume, as demonstrated using a combination of Accelerator Mass Spectroscopy detection and wet chemistry separation methods (Otosaka et al., 2011; Schwehr et al., 2009).

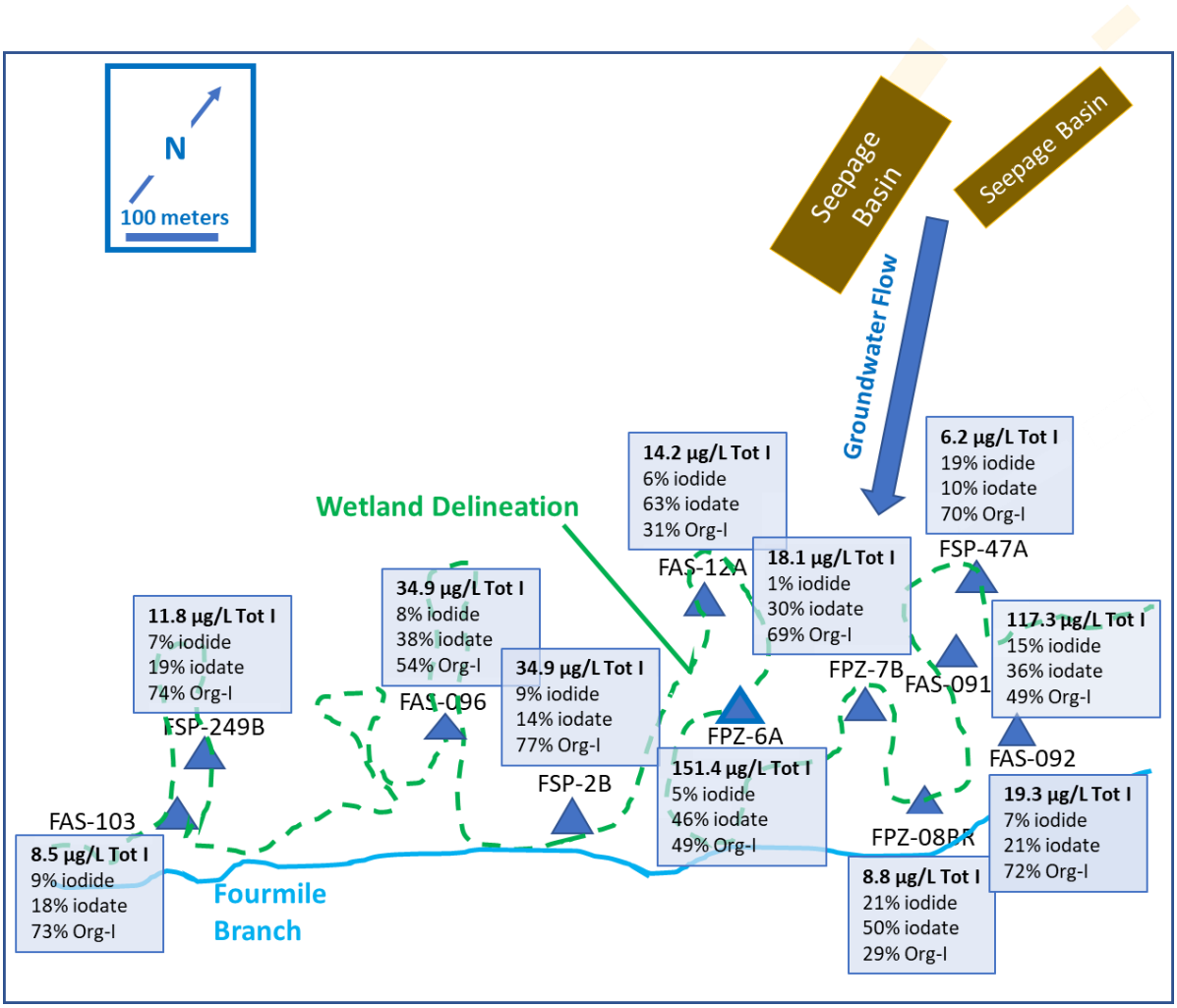

Fig. 6. Iodine speciation in the F-Area wetland. Acidic aqueous waste from operations of the isotope separations facility was released into unlined earthen basins (yellow rectangles) and has migrated into the Fourmile Branch wetland (delineated with a green dashed line). The total ^{127}I and percentage of each of the three measured species are presented for each location. Samples were collected April 2018.

Three of the wells reported in Fig. 6 had total iodine concentrations that approach reported regional background levels of ~8 µg/L (Otosaka et al., 2011) (FAS-103, FSP-47A, and FPZ-08BR), while the others were impacted by the contaminant plume. The well with the highest iodine concentration was FPZ-6A, which is the same well that was repeatedly used to monitor iodine speciation changes as a function of seasons (Table 1). The average distribution of iodine species in Fig. 6 was 13 ± 9% I^-, 27 ± 18% IO_3^-, and 60 ± 22% org-I. There is no apparent

consistent spatial trend of iodine speciation with respect to proximity to the stream. Otosaka et al. (2011) observed a gradual and consistent shift in iodine speciation whereby almost all the iodine near the source was I^- and as the plume progressed towards the wetland, progressively more IO_3^- and org-I were formed, and by the time the plume reached the wetland, it was approximately 70% org-I.

Regression analyses were conducted between total iodine, I^-, IO_3-, and org-I, presented in Figure 6 and several other groundwater chemical parameters (pH, ORP, DOC, total N, Fe, alkalinity, nitrate, tritium, and turbidity) (Table 2). Total ^{129}I was very strongly correlated to total ^{127}I, DOC, and turbidity. The correlation with turbidity, which is a measure of particles that can diffract light, and DOC, a measure of organic carbon concentrations that can pass a 0.45 μm membrane, suggest that some iodine may be associated with organic compounds (org-I) and/or inorganic particles. Xu et al. (2011b) reported that a significant fraction of dissolved iodine in the Fourmile Branch wetland is strongly bound to mineral or organic particles. In Table 2, there were no significant iodine correlations with pH or ORP, two governing parameters that have been shown in laboratory studies to be critical to iodine aqueous concentration in wetland sediment systems (Emerson et al., 2014). The correlations of iodine with NO_3^-/NO_2^- as N (and total N) and tritium concentrations reflect that all three solutes were contaminants. While the biogeochemistry of tritium is relatively simple in that it is a conservative trace of water, it has a relatively short radiological decay (half-life = 12.3 years) and would be expected to have undergone a couple half-lives since being released 40 to 60 years ago into the seepage basins. Nitrate has a far more complicated biogeochemistry than tritium, including undergoing redox changes that may promote binding to sediments (e.g., NH_4^+) or volatilization (e.g., N_2), and it is consumed by microbes and plants. However, at the extremely high nitrate levels in the plume

(Table 2), most of the nitrate originated from the HNO_3 disposed in the basins, and much of the large mass of NO_3^- likely swamped many biogeochemical processes that typically occur, resulting in it traveling through the system as a conservative tracer, similar to tritium. No significant correlations were observed with Fe concentrations and alkalinity (Table 2).

Table 2
Correlation coefficients (*r*) between groundwater chemical properties and iodine species (speciation data presented in Figure 6; samples collected April 2018).

Solute	Units	Minimum	Maximum	Correlation Coefficients (*r*)					
				Total ^{129}I	**Total ^{127}I**	**$^{127}I^-$**	**$^{127}IO_3^-$**	**Org-^{127}I**	**pH**
Total ^{129}I	(Bq/L)	0.038	7.70						
Total ^{127}I	(µg/L)	5.49	151.41	0.883					
$^{127}I^-$	(µg /L)	0.24	15.37	0.887	0.828				
$^{127}IO_3^-$	(µg /L)	0.63	60.57	0.847	0.993	0.786			
Org-^{127}I	(µg /L)	2.6	83.8	0.875	0.996	0.798	0.984		
pH		4.2	7.2	0.186	-0.126	0.144	-0.142	-0.155	
ORP	(mV)	143	332	0.051	0.193	-0.100	0.235	0.204	-0.397
DOC	(mg/L)	0.49	10.64	0.649	0.607	0.486	0.579	0.624	0.228
Total N	(mg/L)	0.39	61.05	0.389	0.729	0.261	0.766	0.753	-0.519
Fe	(mg/L)	0.17	33	-0.258	0.032	-0.100	0.116	-0.009	-0.283
Alkalinity	(mg/L)	0	74	0.392	0.076	0.294	0.055	0.051	0.929
NO_3^-/NO_2^- as N	(mg/L)	1.12	80.1	0.338	0.692	0.223	0.729	0.719	-0.579
Tritium	(Bq/mL)	0.269	29.9	0.411	0.739	0.270	0.772	0.767	-0.490
Turbidity	(NTU)	0.4	32.1	0.589	0.266	0.653	0.200	0.239	0.341

Significant r with 10 degrees of freedom & $p < 0.05$; Critical r = 0.576.
Significant r with 10 degrees of freedom & $p < 0.01$; Critical r = 0.658

Additional significant correlations ($p < 0.01$) not shown include Total N/tritium = 0.998; Nitrate/tritium = 0.992.

5. Conclusions

These results suggest that hydrological and/or biogeochemical processes unique to wetlands, but not present in uplands, are causing the observed contaminant fluctuations. There appears to be multiple processes interacting to produce this response, including seasonal fluctuations in water table height, water temperature, microbiology, and chemistry. During the summer months, the water table decreased, the water temperature increased, and the total iodine concentrations increased. Importantly, other solutes, such as nitrate and tritium, did not follow any seasonal trends, indicating that the fluctuations were not controlled solely by hydrological processes. It was also noted that most of the increase of iodine in the summer months could be attributed to proportional increases in org-I, and not to increases in I^- or IO_3^-.

A coupled hydrological and biogeochemical explanation is proposed to tie these observations together (Fig. 7). Regarding the biogeochemical processes, the seasonal water temperatures in surface water can vary by 15 ºC, which would have a profound impact on microbial activity. Organo-iodine formation, iodination, is almost exclusively a biologically mediated process (Yeager et al., 2017). Furthermore, >95% of the ^{129}I in these systems are associated with the solid phase, and more specifically the organic matter in the soil (Kaplan et al., 2014b). Thus, as the microbes consumed soil organic matter, it is expected that ^{129}I bound to the soil organic matter will be released into the mobile aqueous phase as low molecular weight molecules. Increased summer water temperatures are also expected to promote iodine diffusion from the sediments.

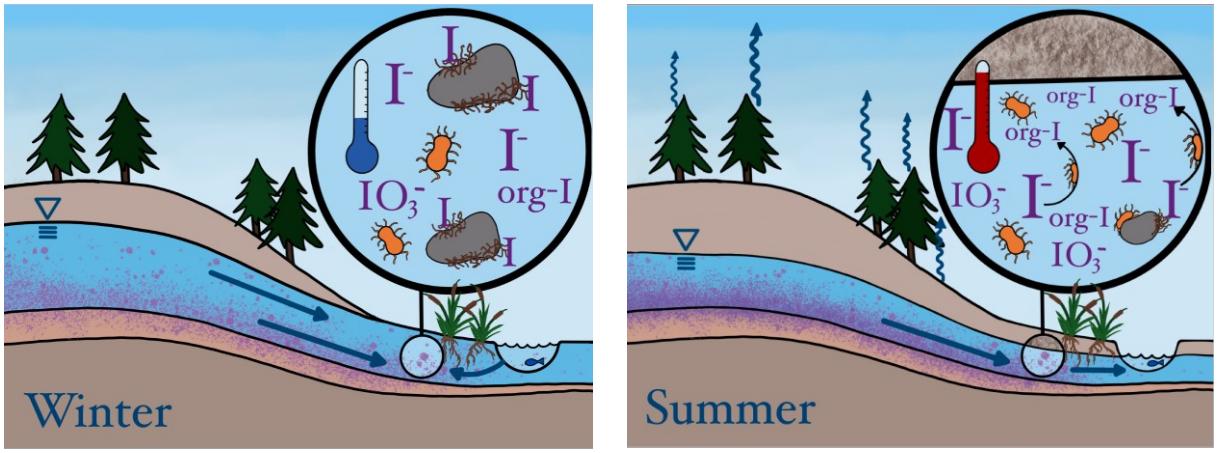

Fig. 7. Schematic of proposed coupled hydrological and biogeochemical processes responsible for seasonal ^{129}I concentration fluctuations. During the summer months, the water table decreased, the water temperature increased, and the total iodine concentrations increased. Most of the increase of iodine in the summer months could be attributed to proportional increases in org-I, and not to I^- or IO_3^-.

There are three potential hydrological processes that may be contributing to the observed iodine seasonal changes. As the water table decreases during the summer months, the remaining water is comprised of a greater proportion of water from the lower depths near the top of the Tan Clay, where the iodine concentrations are greatest. Additionally, during the summer months, the water flow paths may change such that the sampling locations may be intercepting more of the contaminant plume, less of the diluting rainwater due to evapotranspiration by the forested vegetation in the wetland, and less of the diluting water from Fourmile Branch as its height (hydraulic head) decreases during the summer (Rouxel et al., 2011). These results have spurred on-going laboratory studies to systematically change only one parameter, such as water temperature and degree of moisture saturation, while quantifying changes in iodine species, organic matter composition, and microbial community structure. Results from such controlled experiments will permit quantitative modeling of this seasonal response. Together these results underscore the importance of coupled processes influencing contaminant concentrations, and the

need to assess seasonal contaminant variations to optimize long-term monitoring programs of wetlands.

Acknowledgements

This work was supported by the Department of Energy's Subsurface Biogeochemical Research Program within the Office of Science (DE-FG02-08ER64567; DE-SC0021024); SRNL's Laboratory Directed Research and Development program (LDRD-2018-00005); and Savannah River Nuclear Solutions' Area Completion Programs. Work was conducted at the Savannah River National Laboratory under the U.S. Department of Energy Contract DE-AC09-96SR18500. Graphical art was provided by Savannah Kaplan.

References

Ayotte, J. D., Belaval, M., Olson, S. A., Burow, K. R., Flanagan, S. M., Hinkle, S. R., and Lindsey, B. D. (2015). Factors affecting temporal variability of arsenic in groundwater used for drinking water supply in the United States. *Science of the Total Environment* **505**, 1370-1379.

Baird, R. B., Rice, E. W., and Eaton, A. D. (2017). Standard methods for the examination of water and wastewater, 23rd edition. Water Environment Federation, American Public Health Association, American Water Works Association, Washington DC.

Benner, S. G., Polizzotto, M. L., Kocar, B. D., Ganguly, S., Phan, K., Ouch, K., Sampson, M., and Fendorf, S. (2008). Groundwater flow in an arsenic-contaminated aquifer, Mekong Delta, Cambodia. *Applied Geochemistry* **23**, 3072-3087.

Berg, M., Tran, H. C., Nguyen, T. C., Pham, H. V., Schertenleib, R., and Giger, W. (2001). Arsenic contamination of groundwater and drinking water in Vietnam: a human health threat. *Environmental Science & Technology* **35**, 2621-2626.

Biester, H., Selimović, D., Hemmerich, S., and Petri, M. (2006). Halogens in pore water of peat bogs–the role of peat decomposition and dissolved organic matter. *Biogeosciences* **3**, 53-64.

Cotton, F. A., Wilkinson, G., Murillo, C. A., Bochmann, M., and Grimes, R. (1988). "Advanced inorganic chemistry," Wiley New York.

Denham, M., and Vangelas, K. M. (2008). Biogeochemical gradients as a framework for understanding waste-site evolution. *Remediation* **19**, 5-17.

573 Denham, M. E. (1995). "SRS Geology/Hydrogeology Environmental Information Document,"
574 Rep. No. WSRC-TR-95-0046. Westinghouse Savannah River Company, Aiken, SC.
575 Denham, M. E., and Amidon, M. B. (2016). "Analysis of concentration versus time trends for
576 select contaminants in groundwater and wetland surface water associated with the F-Area
577 and H-Area seepage basins," Rep. No. SRNL-STI-2016-00558. Savannah River National
578 Laboratory, Aiken, SC.
579 DOE-LM (2012). "Evaluation of Groundwater Constituents and Seasonal Variation at the
580 Riverton, Wyoming, Processing Site," Rep. No. LMS/RVT/S08364. U.S. Department of
581 Energy-Legacy Management, Washington, DC.
582 Efstathiou, M., Aristarchou, T., Kiliari, T., Demetriou, A., and Pashalidis, I. (2014). Seasonal
583 variation, chemical behavior and kinetics of uranium in an unconfined groundwater
584 system. *Journal of Radioanalytical and Nuclear Chemistry* **299**, 171-175.
585 Emerson, H. P., Xu, C., Feng, Y., Lilley, M., Kaplan, D. I., Santschi, P. H., and Powell, B. A.
586 (2014). Geochemical controls of iodine transport in Savannah River Site subsurface
587 sediments. *Chemical Geology* **45**, 105-113.
588 EPA (2001). "Radionuclides rule: A quick reference guide," Rep. No. EPA-816-F-01-003. U.S.
589 Environmental Protection Agency, Washington, DC.
590 EPA (2009). "Technical Notes for EPA Method 901.1, Gamma Emitting Radionuclides in
591 Drinking Water," Rep. No. EPA 901.1. U.S. EPA, Washington, DC.
592 EPA (2019a). "Analytical Methods Approved for Drinking Water Compliance Monitoring of
593 Inorganic Contaminants and Other Inorganic Constituents," Rep. No. DPA 815-B-19-
594 002. U.S. Environmental Protection Agency, Washington DC.
595 EPA (2019b). "Analytical Methods Approved for Drinking Water Compliance Monitoring of
596 Radionuclides," Rep. No. EPA 815-B-19-004. U.S. Environmental Protection Agency,
597 Washington DC.
598 Fuge, R., and Johnson, C. C. (1986). The geochemistry of iodine—a review. *Environmental*
599 *Geochemistry and Health* **8**, 31-54.
600 IAEA (2007). "Estimation of global inventories of radioactive waste and other radioactive
601 materials," Rep. No. IAEA-TECDOC-1591. International Atomic Energy Agency,
602 Vienna, Austria.
603 Kaplan, D. I. (2021). "Geochemical Data Package for Performance Assessment Calculations
604 Related to the Savannah River Site," Rep. No. SRNL-STI-2021-00017. Savannah River
605 National Laboratory, Aiken, SC.
606 Kaplan, D. I., Denham, M. E., Zhang, S., Yeager, C., Xu, C., Schwehr, K. A., Li, H. P., Ho, Y.
607 F., Wellman, D., and Santschi, P. H. (2014a). Radioiodine biogeochemistry and
608 prevalence in groundwater *Critical Reviews in Environmental Science and Technology*
609 **44**, 2287-2337.
610 Kaplan, D. I., Zhang, S., Roberts, K. A., Schwehr, K., Xu, C., Creeley, D., Ho, Y.-F., Li, H.-P.,
611 Yeager, C. M., and Santschi, P. H. (2014b). Radioiodine concentrated in a wetland.
612 *Journal of Environmental Radioactivity* **131**, 57-61.
613 Killian, T. H., Kolb, N. L., Corbo, P., and Marine, I. W. (1987a). "F-Area Seepage Basins," Rep.
614 No. SPST-85-704, E. I. du Pont de Nemours & Co., Savannah River Laboratory, Aiken,
615 SC.
616 Killian, T. H., Kolb, N. L., Corbo, P., and Marine, I. W. (1987b). "H-Area Seepage Basins," Rep.
617 No. DPST-85-706. E. I. du Pont de Nemours & Co, Aiken, SC.

Kumar, A. R., and Riyazuddin, P. (2011). Speciation of selenium in groundwater: Seasonal variations and redox transformations. *Journal of Hazardous Materials* **192**, 263-269.

Li, H.-P., Brinkmeyer, R., Jones, W. L., Zhang, S., Xu, C., Ho, Y.-F., Schwehr, K. A., Kaplan, D. I., Santschi, P. H., and Yeager, C. M. (2012a). Iodide Oxidizing Activity of Bacteria from Subsurface Sediments of the Savannah River Site. *In* "Interdisciplinary Studies on Environmental Chemistry Vol. 6 - Environmental Pollution and Ecotoxicology" (K. M. M. Kawaguchi, H. Sato, T. Yokokawa, T. Itai, T. M. Nguyen, J. Ono, S. Tanabe, ed.), Vol. 6, pp. 89-97, Terra Scientific Publishing Company, Tokyo.

Li, H.-P., Brinkmeyer, R., Jones, W. L., Zhang, S., Xu, C., Schwehr, K. A., Santschi, P. H., Kaplan, D. I., and Yeager, C. M. (2011). Iodide accumulation by aerobic bacteria isolated from subsurface sediments of a I-129-contaminated aquifer at the Savannah River Site, South Carolina. *Applied and Environmental Microbiology* **77**, 2153-2160.

Li, H.-P., Daniel, B., Creeley, D., Grandbois, R., Zhang, S., Xu, C., Ho, Y.-F., Schwehr, K. A., Kaplan, D. I., and Santschi, P. H. (2014). Superoxide production by a manganese-oxidizing bacterium facilitates iodide oxidation. *Applied and Environmental Microbiology* **80**, 2693-2699.

Li, H.-P., Yeager, C. M., Brinkmeyer, R., Zhang, S., Ho, Y.-F., Xu, C., Jones, W. L., Schwehr, K. A., Otosaka, S., Roberts, K. A., Kaplan, D. I., and Santschi, P. H. (2012b). Bacterial production of organic acids enhances H_2O_2-dependent iodide oxidation. *Environmental Science & Technology* **46**, 4837-4844.

Liu, Y., and von Gunten, H. R. (1988). "Migration chemistry and behaviour of iodine relevant to geological disposal of radioactive wastes. A literature review with a compilation of sorption data," Rep. No. PSI-16. Paul Scherrer Institute, Wuerenlingen, Switzerland.

Meyer, A. M., Klein, C., Fünfrocken, E., Kautenburger, R., and Beck, H. P. (2019). Real-time monitoring of water quality to identify pollution pathways in small and middle scale rivers. *Science of the Total Environment* **651**, 2323-2333.

Moulin, V., and Moulin, C. (2001). Radionuclide speciation in the environment: a review. *Radiochimica Acta* **89**, 773.

Nadakavukaren, J. J., Ingermann, R. L., Jeddeloh, G., and Falkowski, S. J. (1984). Seasonal variation of arsenic concentration in well water in Lane County, Oregon. *Bull. Environ. Contam. Toxicol.;(United States)* **33**, 264–269.

Neeway, J. J., Kaplan, D. I., Bagwell, C. E., Rockhold, M. L., Szecsody, J. E., Truex, M. J., and Qafoku, N. P. (2019). A review of the behavior of radioiodine in the subsurface at two DOE sites. *Science of The Total Environment* **691**, 466-475.

Nichols, R. L., and Dickson, J. O. (2020). "Evaluation of Constituents of Concern above Primary Drinking Water Standards at the F- and H-Area Wetlands (Phase 2b Corrective Action Goal)," Rep. No. SRNL-STI-2019-00234. Savannah River National Laboratory, Aiken, South Carolina.

Orth, D. A. (1963). Plutonium Metal from Trifluoride. *Industrial & Engineering Chemistry Process Design and Development* **2**, 121-127.

Otosaka, S., Schwehr, K. A., Kaplan, D. I., Roberts, D. A., Zhang, S., Xu, C., Li, H.-P., Ho, Y.-F., Brinkmeyer, R., Yeager, C. M., and Santschi, P. H. (2011). Factors controlling mobility of ^{127}I and ^{129}I species in an acidic groundwater plume at the Savannah River Site. *The Science of the Total Environment* **409**, 3857-3865.

Polizzotto, M. L., Kocar, B. D., Benner, S. G., Sampson, M., and Fendorf, S. (2008). Near-surface wetland sediments as a source of arsenic release to ground water in Asia. *Nature* **454**, 505-508.

R Core Team (2021). R: A Language and Environment for Statistical Computing Version 4.1.1. Vol. 2021. R Foundation for Statistical Computing, Vienna, Austria.

R Core Team and Contributors Worldwide (2021). The R Stats Package, Version 4.1.1. The R Foundation for Statistical Computing, Vienna, Austria.

Roszak, D., and Colwell, R. (1987). Survival strategies of bacteria in the natural environment. *Microbiological reviews* **51**, 365-379.

Rouxel, M., Molénat, J., Ruiz, L., Legout, C., Faucheux, M., and Gascuel-Odoux, C. (2011). Seasonal and spatial variation in groundwater quality along the hillslope of an agricultural research catchment (Western France). *Hydrological Processes* **25**, 831-841.

Santschi, P., Xu, C., Zhang, S., Schwehr, K., Lin, P., Yeager, C., and Kaplan, D. I. (2017). Recent Advances in the Detection of Specific Natural Organic Compounds as Carriers for Radionuclides in Soil and Water Environments, with Examples of Radioiodine and Plutonium. *J. Environ. Radioactivity* **171**, 226-233.

Satoh, Y., and Imai, S. (2020). Evaluation of dissolution flux of iodine from brackish lake sediments under different temperature and oxygenic conditions. *Science of The Total Environment* **707**, 135920.

Schaefer, M. V., Ying, S. C., Benner, S. G., Duan, Y., Wang, Y., and Fendorf, S. (2016). Aquifer arsenic cycling induced by seasonal hydrologic changes within the Yangtze River Basin. *Environmental Science & Technology* **50**, 3521-3529.

Schwehr, K. A., Otosaka, S., Merchel, S., Kaplan, D. I., Zhang, S., Xu, C., Li, H. P., Ho, Y. F., Yeager, C. M., and Santschi, P. H. (2014). Speciation of iodine isotopes inside and outside of a contaminant plume at the Savannah River Site. *Science of the Total Environment.* **497/498**, 671-678.

Schwehr, K. A., Santschi, P. H., Kaplan, D. I., Yeager, C. M., and Brinkmeyer, R. (2009). Organo-iodine formation in soils and aquifer sediments at ambient concentrations. *Environmental Science & Technology* **43**, 7258-7264.

Shimamoto, Y. S., Takahashi, Y., and Terada, Y. (2011). Formation of Organic Iodine Supplied as Iodide in a Soil-Water System in Chiba, Japan. *Environmental Science & Technology* **45**, 2086-2092.

Smith, J., Clarke, R., and Bowes, M. (2010). Are groundwater nitrate concentrations reaching a turning point in some chalk aquifers? *Science of the total environment* **408**, 4722-4732.

Sollins, P., Homann, P., and Caldwell, B. A. (1996). Stabilization and destabilization of soil organic matter: mechanisms and controls. *Geoderma* **74**, 65-105.

SRNS (2019). "Annual Corrective Action Report for the F-Area Hazardous Waste Management Facility, the H-Area Hazardous Waste Management Facility, and the Mixed Waste Management Facility," Rep. No. SRNS-RP-2019-00111. Savannah River Nuclear Solutions, Aiken, SC.

Thundiyil, J. G., Yuan, Y., Smith, A. H., and Steinmaus, C. (2007). Seasonal variation of arsenic concentration in wells in Nevada. *Environmental Research* **104**, 367-373.

Wagner, J. C., Peterson, J. L., Mueller, D., Gehin, J. C., Worrall, A., Taiwo, T., Nutt, M., Williamson, M. A., Todosow, M., and Wigeland, R. (2012). "Categorization of used nuclear fuel inventory in support of a comprehensive national nuclear fuel cycle

strategy," Rep. No. ORNL/TM--2012/308. Oak Ridge National Laboratory (ORNL), Oak Ridge, TN.
Xu, C., Chen, H., Sugiyama, Y., Zhang, S., Li, H.-P., Ho, Y.-F., Chuang, C.-Y., Schwehr, K. A., Kaplan, D. I., Yeager, C., Roberts, K. A., Hatcher, P. G., and Santschi, P. H. (2013). Novel molecular-level evidence of iodine binding to natural organic matter from Fourier transform ion cyclotron resonance mass spectrometry. *Science of The Total Environment* **449**, 244-252.
Xu, C., Miller, E. J., Zhang, S., Li, H. P., Ho, Y. F., Schwehr, K. A., Kaplan, D. I., Otosaka, S., Roberts, K. A., Brinkmeyer, R., Yeager, C. M., and Santschi, P. H. (2011a). Sequestration and remobilization of radioiodine (I-129) by soil organic matter and possible consequences of the remedial action at Savannah River Site. *Environmental Science & Technology* **45**, 9975-9983.
Xu, C., Zhang, S., Ho, Y.-F., Miller, E. J., Roberts, K. A., Li, H.-P., Schwehr, K. A., Otosaka, S., Kaplan, D. I., Brinkmeyer, R., Yeager, C. M., and Santschi, P. H. (2011b). Is soil natural organic matter a sink or source for mobile radioiodine (^{129}I) at the Savannah River Site? *Geochimica et Cosmochimica Acta* **75**, 5716-5735.
Xu, C., Zhang, S., Sugiyama, Y., Ohte, N., Ho, Y.-F., Fujitake, N., Kaplan, D. I., Yeager, C. M., Schwehr, K., and Santschi, P. H. (2016). Role of natural organic matter on iodine and ^{239,240}Pu distribution and mobility in environmental samples from the northwestern Fukushima Prefecture, Japan. *Journal of Environmental Radioactivity* **153**, 156-166.
Xu, C., Zhong, J., Hatcher, P. G., Zhang, S., Li, H.-P., Ho, Y.-F., Schwehr, K. A., Kaplan, D. I., Roberts, K. A., Brinkmeyer, R., Yeager, C. M., and Santschi, P. H. (2012). Molecular environment of stable iodine and radioiodine (^{129}I) in natural organic matter: Evidence inferred from NMR and binding experiments at environmentally relevant concentrations. *Geochimica et Cosmochimica Acta* **97**, 166-182.
Yabusaki, S. B., Fang, Y., and Waichler, S. R. (2008). Building conceptual models of field-scale uranium reactive transport in a dynamic vadose zone-aquifer-river system. *Water Resources Research* **44**.
Yamaguchi, N., Nakano, M., Takamatsu, R., and Tanida, H. (2010). Inorganic iodine incorporation into soil organic matter: Evidence from iodine K-edge absorption near-edge structure. *Journal of Environmental Radioactivity* **101**, 451-457.
Yeager, C. M., Amachi, S., Grandbois, R., Kaplan, D. I., Xu, C., Schwehr, K. A., and Santschi, P. H. (2017). Microbial Transformation of Iodine: From Radioisotopes to Iodine Deficiency. *In* "Advances in Applied Microbiology" (S. Sariaslani and G. M. Gadd, eds.), Vol. 101, pp. 83-136. Academic Press.
Zhang, S., Du, J., Xu, C., Schwehr, K. A., Ho, Y. F., Li, H. P., Roberts, K. A., Kaplan, D. I., Brinkmeyer, R., Yeager, C. M., Chang, H. S., and Santschi, P. H. (2011). Concentration-dependent mobility, retardation, and speciation of iodine in surface sediment from the Savannah River Site. *Environmental Science & Technology* **45**, 5543-5549.
Zhang, S., Ho, Y. F., Creeley, D., Roberts, K. A., Xu, C., Li, H. S., Schwehr, K. A., Kaplan, D. I., Yeager, C. M., and Santschi, P. H. (2014). Temporal Variation of Iodine Concentration and Speciation (^{127}I and ^{129}I) in Wetland Groundwater from the Savannah River Site, USA. *Environmental Science & Technology* **48**, 11218-11226.
Zhang, S., Schwehr, K. A., Ho, Y. F., Xu, C., Roberts, K. A., Kaplan, D. I., Brinkmeyer, R., Yeager, C. M., and Santschi, P. H. (2010). A novel approach for the simultaneous determination of iodide, iodate and organo-iodide for I-127 and I-129 in environmental

753 samples using gas chromatography-mass spectrometry. *Environmental Science &*
754 *Technology* **44**, 9042-9048.
755 Zhang, S., Xu, C., Creeley, D., Ho, Y.-F., Li, H.-P., Grandbois, R., Schwehr, K. A., Kaplan, D.
756 I., Yeager, C. M., Wellman, D., and Santschi, P. H. (2013). Iodine-129 and Iodine-127
757 Speciation in Groundwater at the Hanford Site, U.S.: Iodate Incorporation into Calcite.
758 *Environmental Science & Technology* **47**, 9635-9642.
759